How Do Charges Travel through DNA?—An Update on a Current Debate**

Mark W. Grinstaff*

The biological role of deoxyribonucleic acid (DNA) is to store and code genetic information. This unique biopolymer consists of a double helix with major and minor grooves. An aromatic π-stack core runs throughout the structure where the bases of the pyrimidine deoxynucleotides (thymidine, T; cytidine, C) and purine deoxynucleotides (adenosine, A; guanosine, G) participate in Watson–Crick base pairing (A:T; C:G). Although first posed in the 1960s,[1, 2] the question of how charged species can be transported over short or long distance in DNA is still debated.[3–8] An intense worldwide research effort is underway to explain the large variations in observed electron transfer rates (microsecond to picosecond) and to develop well-defined chemical systems for further study.

Radiation, carcinogens, and metabolic waste products can damage DNA, and, if left unrepaired by the normal cellular machinery, these damages can lead to mutations and carcinogenesis with grave health consequences.[9–17] Further analysis reveals many of these damages to be a result of selective radical reactions with guanine bases, consistent with the relative ease with which guanine is oxidized compared to adenine, cytosine, and thymine.[18–23] A study of electron transfer and radical-cation migration in DNA as well as identification of the factors that control the rates of these processes will provide valuable information for understanding DNA damage in vivo and insight into the mechanism of charge transfer through different media. A greater understanding of DNA-mediated electron transfer may have an additional clinical impact through the development of novel diagnostic tools for screening nucleic acids, proteins, or carcinogens.

Although significant advances in the study of charge transport in DNA have been reported within the last five years,[7, 24–26] a number of issues remain unresolved. Current studies address multiple factors affecting this process such as oligonucleotide sequence, base pairing, π stacking, and duplex structure as well as the donor–acceptor distance, the labeling site, and the dynamics. In contrast to-electron transfer through proteins, where the factors controlling electron-transfer rates are more clearly recognized,[27–30] our understanding of charge transport through DNA is limited owing to fewer experimental and theoretical studies. Yet many of the experimental techniques developed for investigating protein-mediated electron transfer and concepts understood with regard to this process can be used to study electron transfer in DNA. A three-pronged approach used to investigate charge transfer in DNA includes 1) labeling DNA with redox probes through intercalation and/or covalent linkages, 2) initiating charge transport by photochemical or electrochemical techniques, and 3) detecting the transfer events by spectroscopic, electrochemical, or biochemical methods. With these tools in hand, experiments are ongoing to further understand the dynamics of DNA-mediated electron transfer and the role of charge-transfer reactions in DNA damage and repair.[31]

Diederichsen's 1997 highlight "Charge Transfer in DNA: A Controversy" describes the limitations and advantages of the first DNA electron-transfer experiments.[3] Electron transfer data from these experiments are summarized in Table 1. Organic and inorganic intercalators were first reported for studying electron transfer in DNA.[32–35] These experiments provide only limited information on electron transfer, given the lack of an accurate measurement of the distance between the donor and acceptor as well as concern for pairing of the donor–acceptor complexes.[36–39] The next advance came with covalently linked donor and acceptor intercalators. Rapid electron transfer between two tethered ruthenium and rhodium intercalators ($[Ru(phen)_2(dppz)]^{2+}$ and $[Rh(phen)(phi)_2]^{3+}$; phen = 1,10-phenanthroline, dppz = dipyrido[2,3-*a*:2′,3′-*c*]phenazine, phi = 9,10-diimine phenanthrenequinone) separated by more than 40 Å in DNA is observed; the lower limit of this electron transfer rate is $10^9\ s^{-1}$. The effect of the medium on this electron transfer is small, since β, which represents the ability of the intervening medium to facilitate electron transfer, is $0.2\ Å^{-1}$.[40] Investigations with the fluorophore stilbene incorporated in a DNA hairpin yield distance-dependent electron-transfer rates spanning from 10^8 to $10^{12}\ s^{-1}$ ($\beta = 0.64\ Å^{-1}$).[41] Similarly, distance-dependent electron transfer is reported between an intercalated acridine and guanine at rates that range from 10^5 to $10^{10}\ s^{-1}$ ($\beta = 1.4\ Å^{-1}$).[42] A relatively slow electron-transfer ($10^6\ s^{-1}$) is measured between two ruthenium complexes that modify the ribose moiety of a DNA duplex.[43] For additional information on these electron-transfer experiments, the reader is referred to

[*] Prof. M. W. Grinstaff
Department of Chemistry, Paul M. Gross Chemical Laboratory
Duke University, Durham, NC 27708 (USA)
Fax: (+1) 919-660-1605
E-mail: mwg@chem.duke.edu

[**] The author greatly appreciates reprints from and his correspondences with Professors Barton, Diederichsen, Giese, Gray, Harriman, Jortner, Lewis, Netzel, Schuster, Tanaka, and Zewail during the preparation of this highlight.

  1433-7851/99/3824-3629 $ 17.50+.50/0

Table 1. The results of studies on DNA-mediated electron transfer.

Donor and acceptor	Covalently attached	d [Å][a]	β	k_{ET} [s^{-1}]	Research group	Year
tethered Ru^{II} and Rh^{III} intercalators	yes	> 40	0.2	10^9	Barton[40]	1993
Ru^{II} and Rh^{III} intercalators	no	–	0.2	10^{10}	Barton[35]	1996
tethered E and Rh^{III} intercalators	yes	17 – 36	–	10^{10}	Barton[52]	1997
A_2, A_s and G, Z	yes	3.4 – 10.2	0.1 – 1.0	$10^9 - 10^{10}$	Barton[54]	1999
daunomycin and Au electrode	yes	10 – 35	–	10^2	Barton/Hill[57]	1999
E intercalator and Z	yes	10 – 17	–	10^{12}	Barton/Zewail[53]	1999
E and MV^{2+}	no	–	–	10^5	Fromherz[32]	1986
E and MV^{2+}, AO and DAP^{2+}	no	10 – 17	1.0	10^8	Harriman[34, 51]	1992, 1999
stilbenedicarboxamide and guanine	yes	4 – 18	0.64	$10^8 - 10^{12}$	Lewis[41]	1997
naphthalene and A	yes	–	–	10^9	Lewis[56]	1999
Ru^{II} and Ru^{III} ribose complexes	yes	27	1.0 – 1.5	10^6	Meade[43]	1995
intercalated acridine and guanine	yes	3 – 10	1.4	$10^5 - 10^{10}$	Tanaka[42, 55]	1998

[a] d = distance between donor and acceptor.

the original articles cited as well as several commentaries[5, 6, 8, 26, 44–47] and theoretical studies.[48, 49]

A theoretical analysis[50] of recently published DNA-mediated charge-transfer reactions provides both insight into the charge-transfer mechanisms (hopping versus superexchange)[49, 50] and a template from which to discuss the reactions summarized below (Tables 1 – 4). A key point in the article concerns charge-transfer donors and acceptors possessing different energetics and thus participating in different mechanisms.[50] The relative energetics of the donor and acceptor with respect to the DNA bridge determine if 1) a one-step superexchange mechanism occurs (characterized by an exponential decay of the charge-transfer rate with distance) or 2) a hopping mechanism occurs (characterized by a weak dependence of the charge-transfer rate on distance). Superexchange occurs when a positive energy gap exists between the lowest electronic state of the excited donor (D*) and the vibronic manifold of the DNA bridge. The hole hopping mechanism, however, occurs when the lowest vibronic state of electronic origin of D* is in resonance with the highly degenerate DNA vibronic manifold. The rate of hopping is controlled by the energetics of the ion-pair states in the DNA manifold.

Table 2. Results of studies on DNA radical-cation migration.

Donor and acceptor	d [Å][a]	Research group
Rh and Ru tethered intercalators and GG	10 – 200	Barton[65–68]
E and GG	17, 44	Barton[69]
acylated A or G and GGG	7 – 54	Giese[59, 71, 72]
riboflavin and GG, GGG	–	Saito[64]
tethered anthraquinone and GG	10 – 200	Schuster[60, 61, 73, 74]

[a] d = distance between donor and acceptor.

Measurements of electron transfer in DNA between discrete donors and acceptors are described first in this highlight, followed by a discussion of photoinduced guanine oxidation and radical-cation transport. The first case study focuses on the DNA-mediated electron transfer between intercalated ethidium (E) and methyl viologen (MV^{2+}; Table 3, entry 1), electrostatically bound to the DNA.[51] In this system MV^{2+} quenches the photoexcited ethidium. Detailed steady-state and time-resolved fluorescence studies of ethidium quenching as a function of MV^{2+} concentration and reaction temperature yields a reorganization energy λ of 0.66 eV and β value of 1.0 $Å^{-1}$ ($k_{ET} = 10^6 - 10^9\ s^{-1}$). The electron transfer rates also decrease dramatically with distance for both quenchers examined (MV^{2+} and *N,N′*-dimethyl-2,9-diazapyrenium (DAP^{2+})). The values of λ and β are similar to those previously determined for protein-mediated electron transfer and electron tunneling. This is the first determination of λ for a DNA-mediated electron-transfer reaction and emphasizes the need for additional studies of tethered intercalators and covalently linked donor – acceptor systems.

When a tethered and intercalated donor and acceptor are at each end of a DNA duplex, the rates and distance dependence of electron transfer are dramatically different. In this next study of DNA-mediated electron transfer, the ethidium donor transfers an electron to the $[Rh(phi)_2(bpy)]^{3+}$ (bpy = 2,2′-bipyridyl) acceptor upon photoexcitation (Table 4, entry 1; $k_{ET} = 10^{10}\ s^{-1}$).[52] Systematic variations of the ethidium – Rh^{III} distance from 17 to 36 Å do not substantially alter the quenching of the ethidium fluorescence; however, changes in the sequence do. For example, introduction of a cytosine – adenine mismatch in the modified duplex dramatically reduces the ability of the Rh^{III} center to quench the ethidium fluorescence. These results stress the importance of a well-defined duplex structure for facile electron transfer.

A recent report describes the femtosecond electron transfer between an intercalated and tethered acceptor and a nucleobase donor.[53] The acceptor, ethidium, is at the 5′-end of a DNA duplex, while the electron donor, deazaguanine (Z), is at various oligonucleotide positions 10 to 17 Å from the ethidium (Table 3, entry 2). In this investigation, transient absorption and fluorescence upconversion experiments were used to directly measure ultrafast electron transfer in DNA. Quenching of the photoexcited intercalated ethidium by Z occurs within about 5 ps. This fast electron transfer is the first step to the DNA bridge in a hopping mechanism. A second slower component is also present and attributed to movement of the intercalated ethidium in DNA. This molecular motion reflects the need for the ethidium to preorganize in order to participate in the electron transfer

  1433-7851/99/3824-3630 $ 17.50+.50/0

Table 3. Recently studied organic donors and acceptors.

Entry	Donor	Acceptor	Ref.
1	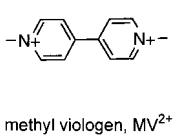 methyl viologen, MV^{2+}	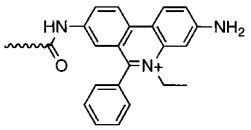 ethidium, E	[34, 51]
2	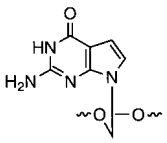 deazaguanine, Z	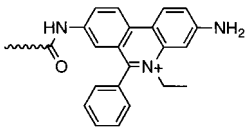 ethidium, E	[53]
3	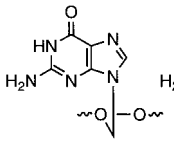 guanine, G 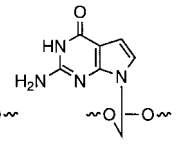 deazaguanine, Z 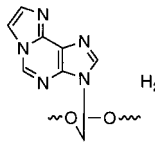 1,*N*6-ethenoadenine, A_ε 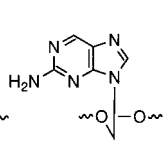 2-aminopurine, A_2		[54]
4	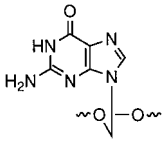 guanine, G	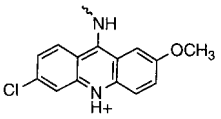 acridine	[42, 55]
5	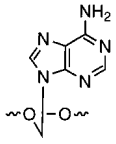 adenosine, A	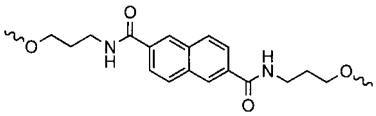 naphthalenedicarboxamide	[56]
6	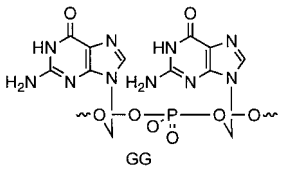 GG	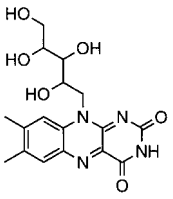 riboflavin	[64]
7	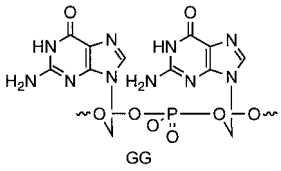 GG	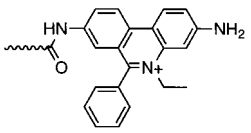 ethidium, E	[69]
8	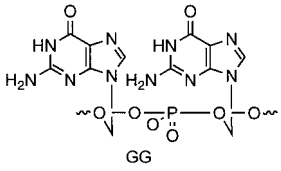 GG	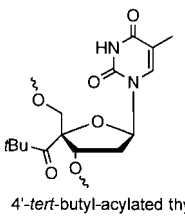 4'-*tert*-butyl-acylated thymidine	[71, 72]
9	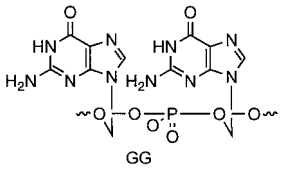 GG	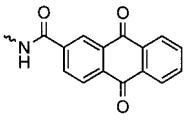 anthraquinone, AQ	[73, 74]

reaction. The electron-transfer rate does not vary significantly with distance; only the yield of quenched ethidium varies. The implications of these results are significant since DNA base dynamics may control the electron-transfer, suggesting that β may not be the best parameter to describe DNA-mediated electron transfer.

The results described above are strikingly different between the tethered and nontethered ethidium electron-transfer systems. In the first system described (intercalated ethidium and surface-bound MV^{2+}; Table 3, entry 1) the electron-transfer rate shows a significant distance dependence over short distances (3–17 Å). Yet fast electron-transfer occurs over longer distances between the covalently tethered ethidium and rhodium(III) complex (Table 4, entry 1). The electron-transfer rates are relatively insensitive to distance (17–36 Å) but sensitive to oligonucleotide sequence. Is this discrepancy a result of different electron-transfer dynamics, the locations of donor and acceptor, or oligonucleotide sequences/structures? Future experiments are needed to explain this apparent discrepancy, and to assess which factors control the electron-transfer rate.

Measurements between fluorescent analogues of adenine (2-aminopurine (A_2) and 1,*N*6-ethenoadenine (A_ε)) and guanine (G) and deazaguanine (Z; Table 3, entry 3) further explore the effect of oligonucleotide structure on the electron-transfer rate.[54] In this system, one oligonucleotide strand of the duplex contains both the donor (G or Z) and acceptor (A_2 or A_ε), which are separated by 3.4, 6.8, and 10.2 Å. Steady-state emission and time-correlated single-photon counting experiments show that quenching of G by A_ε occurs on the time scale of $10^9\ s^{-1}$ ($\beta = 1.0\ Å^{-1}$). In contrast, quenching of G by A_2 occurs even faster ($>10^{10}\ s^{-1}$) and β is closer to $0.1\ Å^{-1}$. Even though the energetics of both these electron-transfer reactions are similar, the electron-transfer rates and β values are different. Structural studies on oligonucleotides containing A_2 and A_ε show that A_2 participates in normal Watson–Crick base pairing, while the bulky A_ε adopts a poorly stacked conformation. These data reveal that structural changes in the base stack influence electron-transfer rates.

  1433-7851/99/3824-3631 $ 17.50+.50/0

Table 4. Recently studied inorganic donors and acceptors.

Entry	Donor	Acceptor	Ref.
1	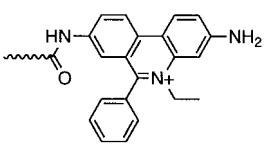 ethidium, E	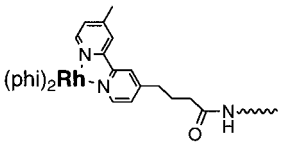 $[Rh(phi)_2(bpy)]^{3+}$	[52]
2	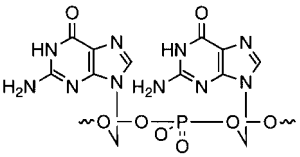 GG	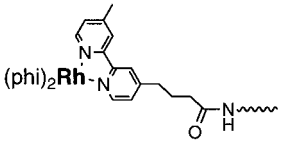 $[Rh(phi)_2(bpy)]^{3+}$	[65 – 68]
3	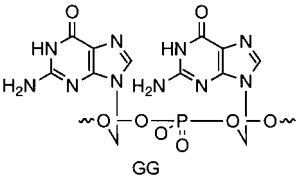 GG	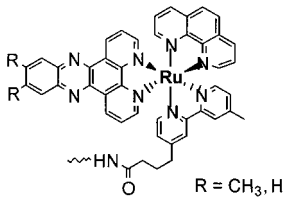 $[Ru(bpy)(phen)(dppz)]^{3+}$	[65 – 68]
4	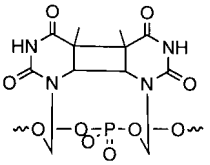 thymine dimer	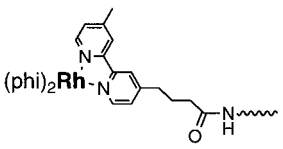 $[Rh(phi)_2(bpy)]^{3+}$	[31]

A recent report describes the distance-dependent electron transfer between a photoexcited acridine and guanine (Table 3, entry 4).[55] In this study, a derivatized 2-methoxyacridine substitutes a nucleobase position in an oligonucleotide. Quenching of the acridine excited state occurs by an adjacent guanine. Rate constants for the forward electron transfer vary from 10^5 to $10^{10}\ s^{-1}$ as the distance increases from 3 to 10 Å. The β value of 1.47 $Å^{-1}$ is in agreement with an earlier value reported from static fluorescence measurements.[42] There is no directional anisotropy for DNA-mediated electron transfer, since the electron transfer rates are similar in both the 5′ and 3′ directions. These data are also consistent with a superexchange mechanism occurring between acridine and guanine.

Similar to earlier work reported on stilbenedicarboxamide hairpins,[41] where superexchange is likely the electron transfer mechanism, an incorporated naphthalene can be used to probe DNA-mediated electron transfer in several novel DNA-hairpin structures.[56] The naphthalene serves as a bridgehead unit in these hairpins, which are synthesized with an automated DNA synthesizer. Quenching of the naphthalene-excited state in the hairpin by an adjacent adenosine (A) occurs swiftly with a rate constant of $10^9\ s^{-1}$ (Table 3, entry 5).

To characterize ground-state electron transfer in DNA, as opposed to photoinitiated electron transfer, a recent report describes electron transfer in well-defined DNA duplex assemblies bound to gold electrodes.[57] The DNA duplexes modified at a specific guanine base with daunomycin are used to probe this ground-state electron-transfer reaction between the redox-active quinone of daunomycin to the gold electrode. The relatively slow electron-transfer rate ($10^2\ s^{-1}$) estimated from the electrochemical data is insensitive to the distance between the redox partners. However, the electron-transfer rate is sensitive to an intervening single base mismatch, which "shuts off" the electron transfer to the gold electrode. The sensitivity of the reaction to base stacking but not to distance suggests that the rate-determining step is not electron transfer through the π stack, but instead electron tunneling through the σ linker to the gold electrode.

A new experimental approach to measure the electrical conducting properties of DNA uses a low-energy electron point source (LEEPS) microscope.[58] Under ultrahigh vacuum conditions, the electrical current of the DNA fibers are directly measured as a function of applied potential. Resistivity values calculated from these measurements are comparable to those of conducting polymers. Excitingly, these measurements are made over very large distances (600 nm or more); photoinduced experiments typically measure electron-transfer rates over distances of less than 5 nm. These results further support the hypothesis that charges can propagate over large distances in DNA.

The measured rates of electron transfer in DNA are remarkably different as summarized above and described in earlier reports (see Table 1). Do non-intercalator donors and acceptors access the DNA π stack? Does the linker from the donor or acceptor to DNA control the rate? Are the rate differences a consequence of different reaction mechanisms? To what degree do different local duplex microstructures (sequences) modulate electron-transfer rates? Is the strong distance dependence previously observed in some systems a consequence of duplex structure or energetics? Additional studies are needed to discern the effect of donor and acceptor site and DNA microstructures on electron-transfer rates. The ability of DNA to facilitate or inhibit long-range electron transfer is significant with regard to the mechanism of oxidative DNA damage.

Oxidative damage in DNA is of utmost importance, and a means to study this biologically relevant process may lead to a better understanding of DNA damage in vivo. Characterizing guanine oxidation in DNA is possible, since photoinduced triggers can initiate this charge-transfer reaction. In these experiments a hole-hopping (or phonon-assisted polaron) mechanism is proposed whereby the photoinduced radical cation (i.e., the hole) moves in a stepwise fashion from one low-energy site in DNA to another.[4, 50, 59–63] This mechanism is consistent with the energies of the donor and acceptor being comparable to the energy levels of the intervening DNA bridge. Since the energy of the radical cation is lowest on G (compared to A, C, and T), the radical cation will localize on

  1433-7851/99/3824-3632 $ 17.50+.50/0

G as it traverses the DNA from one G to another. This radical cation does not possess sufficient energy to reside on the other bases; therefore it must jump to the next G in one complete step (a coherent superexchange transfer). The intervening sequence and distance between the guanine bases affects the electron-transfer rate. In this scenario, a radical cation migrates over large distances in DNA. Recent ab initio calculations of ionization potentials of guanine in B-DNA duplexes reveal that sequences adjacent to guanine affect the ionization potential of guanine.[64] Thus, some local regions of DNA are more likely than others to facilitate radical-cation migration.

Experimental conformation of long-range oxidative damage in DNA requires the use of site specifically labeled probes with well-defined photochemical reactivity. For example, both Rh^{III}($*Rh^{III}$) and Ru^{III} metallointercalators oxidize guanine over extended distances of 60 base pairs (200 Å).[65–68] After irradiation of the intercalated metal complex, gel electrophoresis identifies the oxidized guanine at a 5′-GG-3′ site (Table 4, entries 2 and 3). The yield of oxidized guanine varies slightly with distance for both tethered metallointercalators. In addition, the efficiency of this guanine oxidation is sensitive to sequence. For example, sequences composed of 5′-TA-3′ regions are particularly poor conduits compared to 5′-AA-3′ regions. The ability of a DNA–protein assembly to alter the local microstructure of DNA also affects guanine oxidation by the $*Rh^{III}$ complex.[69] Additionally, a tethered ethidium intercalator yields similar results, indicating that guanine oxidation is not particular to metallointercalators.[70] The lack of an apparent strong dependence on distance in these oxidation reactions, combined with the observation that these charge-transfer reactions are dependent on sequence as well as sensitive to the integrity of the π stack, mirrors the results of previous electron-transfer reactions between metallointercalator complexes.

Photoinitiated radical-cation migration in DNA with subsequent guanine oxidation can also occur using an incorporated 4′-*tert*-butyl-acylated thymidine (Table 3, entry 8) or guanine.[4, 59, 71, 72] A Norrish type I cleavage occurs upon photolysis, generating a radical cation on the ribose of a DNA duplex. This radical cation then migrates to the guanine on the complimentary strands, where DNA strand scission occurs as a result of $G^{+\bullet}$ formation. The radical cation is transported over both short (7–17 Å) and long distances (54 Å), and the efficiency of charge transfer over 54 Å is similar to that over 10 Å. The relative intensity ratios of the cleaved sequences (GGG/$G^{+\bullet}$) yield the relative rate constant data. The calculated value for β is 0.7 $Å^{-1}$ for this biologically relevant charge-transfer reaction. The intervening sequence between the radical cation and the GGG units influences this process substantially, and a simple change from 5′-AT-3′ to 5′-GC-3′ increases the cleavage yield by two orders of magnitude. These results confirm that long-range radical-cation transport can occur by a multistep hopping process.[71]

A recent report describes the influence of nucleotides adjacent to guanine to modulate its reactivity towards oxidative damage.[64] In this study of photoinduced one-electron guanine oxidation, a nontethered riboflavin accepts an electron from duplexes containing the 5′-XGY-3′ sequence (X, Y = A, C, G, and T; see, for example, Table 3, entry 6). The efficiency of GG cleavage occurs in the following order: GGG > CGG > AGG = TGG > TGT, with pyrimidine-G-pyrimidine being the least reactive. Calculations on the same sequences support this experimental result since the ionization potentials are lower (highest oxidative reactivity) for purine-G-purine sequences than for pyrimidine-G-pyrimidine sequences.

Long-distance (200 Å) radical-cation transport also occurs in an AQ-linked DNA duplex (AQ = anthraquinone; Table 3, entry 9) containing four separate GG blocks.[73] Irradiation of the tethered anthraquinone leads to electron transfer and formation of the anthraquinone radical anion and guanine radical cation.[20, 73, 74] Photoinduced radical-cation cleavage of DNA occurs at GG steps adjacent to and remote from the tethered AQ. The distance dependence for guanine oxidation between AQ and the GG steps is minimal. A linear relationship between the log of the GG-cleavage efficiency and the distance between the AQ and the radical cation indicates that the intervening sequence does not significantly influence radical-cation migration.

Radical-cation migration to guanine occurs over long distances with intercalator, 5′-terminal phosphate, and 4′-ribose probes. Yet the efficiency of oxidized guanine is not the same in all cases. Additional experiments need to account for these differences and identify the factors that govern this reaction. Moreover, the data are seemingly contradictory on the effect of sequence on the charge-transfer rate. Future studies must address this issue and quantify the effects of different sequences and mismatches on radical-cation transport. The biological implications of this long-range charge transfer are significant with regard to the extent that a radical cation can propagate in DNA and induce oxidative damage.

The current electron transfer and radical-cation migration systems differ in a number of ways: the specific donors and acceptors, the driving force (ΔG^0) of the electron-transfer reaction, the energetics of donor and acceptor relative to the DNA bridge, the distances between the donor and acceptor, the manner in which the donor and acceptor are covalently linked to (or intercalated in) the oligonucleotide duplex, the sequences, and the local duplex microstructures. Many of these critical issues are highlighted throughout the text; however, additional key points remain at large or unanswered. First, the number of new spectroscopic or electrochemical probes reported in the literature is small. The current repertoire of probes available for study must be expanded to include those that can further explore the dynamics and energetics of charge transfer in DNA.[75–77] Second, the need for NMR studies of solutions or X-ray crystal structures of oligonucleotide duplexes labeled with the donor and acceptor is strikingly evident. Recent NMR solution structure studies on an intercalated Rh–oligonucleotide model system provide the first structural information.[78] Third, the dependence of ΔG^0 on the DNA-mediated charge transfer is unknown. Fourth, the electronic coupling and reorganization energy for tethered intercalators and covalently bound donors and acceptors remains elusive. As was done previously for protein-mediated electron transfer,[28]

  1433-7851/99/3824-3633 $ 17.50+.50/0

these data can be experimentally determined by measuring the rate of charge transfer between the donors and acceptors as a function of driving force and temperature, when the thermodynamic data (ΔG^0, ΔS^0, and ΔH^0) for the charge-transfer reaction are known. Fifth, understanding the dynamics of charge transfer is critical, and additional femtosecond experiments on site specifically labeled DNA are needed to explore the first event(s) in DNA-mediated charge transfer. Finally, the number of theoretical studies reported is limited. New DNA-mediated charge-transfer systems need to be proposed and experimentally tested.

This highlight is intended to briefly summarize new results, stimulate critical discussions, and pique scientific interest. Moreover, it is an invitation to the general scientific community to examine this exciting area of DNA-mediated charge transfer.

German version: *Angew. Chem.* **1999**, *111*, 3845 – 3851

Keywords: DNA oxidation · DNA repair · electron transfer · intercalations

[1] D. D. Eley, D. I. Spivey, *Faraday Soc. Trans.* **1962**, *58*, 411 – 415.
[2] T. A. Hoffman, J. Ladik, *Adv. Chem. Phys.* **1964**, *7*, 84 – 158.
[3] U. Diederichsen, *Angew. Chem.* **1997**, *109*, 2411 – 2413; *Angew. Chem. Int. Ed. Engl.* **1997**, *36*, 2317 – 2319.
[4] M. Ratner, *Nature* **1999**, *397*, 480 – 481.
[5] N. J. Turro, J. K. Barton, *J. Biol. Inorg. Chem.* **1998**, *3*, 201 – 209.
[6] E. K. Wilson, *Chem. Eng. News* **1997**, *75*(8), 33 – 35.
[7] T. L. Netzel in *Organic and Inorganic Photochemistry* (Eds.: V. Ramamurthy, K. S. Schanze), Marcel Dekker, New York, **1998**, pp. 1 – 54.
[8] G. Taubes, *Science* **1997**, *275*, 1420 – 1421.
[9] E. C. Friedberg, G. C. Walker, W. Seide, *DNA Repair and Mutagenesis*, ASM Press, Washington DC, **1995**.
[10] T. Melvin, S. W. Botchway, A. W. Parker, P. O'Neill, *J. Am. Chem. Soc.* **1996**, *118*, 10031 – 10036.
[11] P. O'Neill, E. M. Fielden, *Adv. Radiat. Biol.* **1993**, *17*, 53 – 120.
[12] J. Cadet, *DNA Adducts: Identification and Significance*, IARC, Lyon, France, **1994**.
[13] B. Demple, L. Harrison, *Annu. Rev. Biochem.* **1994**, *63*, 915 – 948.
[14] S. Loft, H. E. Poulsen, *J. Mol. Med.* **1996**, *74*, 297 – 312.
[15] D. M. Close, *Radiat. Res.* **1993**, *135*, 1 – 15.
[16] V. Michalik, *Int. J. Radiat. Biol.* **1992**, *62*, 9 – 20.
[17] M. Bien, H. Steffen, D. Schulte-Frohlinde, *Mutat. Res.* **1988**, *194*, 193 – 205.
[18] S. Steenken, S. V. Jovanovic, *J. Am. Chem. Soc.* **1997**, *119*, 617 – 618.
[19] I. Saito, M. Takayama, H. Sugiyama, K. Nakatani, A. Tsuchida, M. Yamamoto, *J. Am. Chem. Soc.* **1995**, *117*, 6406 – 6407.
[20] B. Armitage, *Chem. Rev.* **1998**, *98*, 1171 – 1200.
[21] C. A. M. Seidel, A. Schulz, M. H. M. Sauer, *J. Phys. Chem.* **1996**, *100*, 5541 – 5553.
[22] H. Sugiyama, I. Saito, *J. Am. Chem. Soc.* **1996**, *118*, 7063 – 7068.
[23] F. Prat, K. N. Houk, C. S. Foote, *J. Am. Chem. Soc.* **1998**, *120*, 845 – 846.
[24] S. O. Kelley, J. K. Barton in *Metal Ions in Biological Systems, Vol. 36* (Eds.: A. Sigel, H. Sigel), Marcel Dekker, New York, **1999**, pp. 211 – 249.
[25] R. E. Holmlin, P. J. Dandliker, J. K. Barton, *Angew. Chem.* **1997**, *109*, 2830 – 2848; *Angew. Chem. Int. Ed. Engl.* **1997**, *36*, 2714 – 2730, and references therein.
[26] T. L. Netzel, *J. Biol. Inorg. Chem.* **1998**, *3*, 210 – 214.
[27] H. B. Gray, J. R. Winkler, *Annu. Rev. Biochem.* **1996**, *65*, 537 – 561.
[28] J. R. Winkler, H. B. Gray, *Chem. Rev.* **1992**, *92*, 369 – 379.
[29] G. McLendon, *Acc. Chem. Res.* **1988**, *21*, 160 – 167.
[30] S. S. Isied, A. Vassilian, *J. Am. Chem. Soc.* **1984**, *106*, 1726 – 32.
[31] P. J. Dandliker, R. E. Holmlin, J. K. Barton, *Science* **1997**, *275*, 1465 – 1468.
[32] P. Fromherz, B. Rieger, *J. Am. Chem. Soc.* **1986**, *108*, 5361 – 5362.
[33] J. K. Barton, C. V. Kumar, N. J. Turro, *J. Am. Chem. Soc.* **1986**, *108*, 6391 – 6393.
[34] A. M. Brun, A. Harriman, *J. Am. Chem. Soc.* **1992**, *114*, 3656 – 3660.
[35] M. R. Arkin, E. D. A. Stemp, R. E. Holmlin, J. K. Barton, A. Hörmann, E. J. C. Olson, P. F. Barbara, *Science* **1996**, *273*, 475 – 480.
[36] P. Lincoln, E. Tuite, B. Nordén, *J. Am. Chem. Soc.* **1997**, *119*, 1454 – 1455.
[37] E. J. C. Olson, D. Hu, A. Hörmann, P. F. Barbara, *J. Phys. Chem. B* **1997**, *101*, 299 – 303.
[38] S. J. Franklin, C. R. Treadway, J. K. Barton, *Inorg. Chem.* **1998**, *37*, 5198 – 5210.
[39] E. K. Erkkila, T. D. Odom, J. K. Barton, *Chem. Rev.* **1999**, *99*, 2777 – 2795.
[40] C. J. Murphy, M. R. Arkin, Y. Jenkins, N. D. Ghatlia, S. H. Bossmann, N. J. Turro, J. K. Barton, *Science* **1993**, *262*, 1025 – 1029.
[41] F. D. Lewis, R. Wu, Y. Zhang, R. L. Letsinger, S. R. Greenfield, M. R. Wasielewski, *Science* **1997**, *277*, 673 – 676.
[42] K. Fukui, K. Tanaka, *Angew. Chem.* **1998**, *110*, 167 – 170; *Angew. Chem. Int. Ed.* **1998**, *37*, 158 – 161.
[43] T. J. Meade, J. F. Kayyem, *Angew. Chem.* **1995**, *107*, 358 – 360; *Angew. Chem. Int. Ed. Engl.* **1995**, *34*, 352 – 354.
[44] T. L. Netzel, *J. Chem. Educ.* **1997**, *74*, 646 – 651.
[45] S. Priyadarshy, S. M. Risser, D. N. Bertan, *J. Biol. Inorg. Chem.* **1998**, *3*, 196 – 200.
[46] F. D. Lewis, R. L. Letsinger, *J. Biol. Inorg. Chem.* **1998**, *3*, 215 – 221.
[47] E. S. Krider, T. J. Meade, *J. Biol. Inorg. Chem.* **1998**, *3*, 222 – 225.
[48] S. Priyadarshy, S. M. Risser, D. N. Beratan, *J. Phys. Chem.* **1996**, *100*, 17678 – 17682.
[49] D. N. Beratan, S. Priyadarshy, S. M. Risser, *Chem. Biol.* **1997**, *4*, 3 – 8.
[50] J. Jortner, M. Bixon, T. Langenbacher, M. E. Michel-Beyerle, *Proc. Natl. Acad. Sci. USA* **1998**, *95*, 12759 – 12765.
[51] A. Harriman, *Angew. Chem.* **1999**, *111*, 996 – 1000; *Angew. Chem. Int. Ed.* **1999**, *38*, 945 – 949.
[52] S. O. Kelley, R. E. Holmlin, E. D. A. Stemp, J. K. Barton, *J. Am. Chem. Soc.* **1997**, *119*, 9861 – 9870.
[53] C. Wan, T. Fiebig, S. O. Kelly, C. R. Treadway, J. K. Barton, A. H. Zewail, *Proc. Natl. Acad. Sci. USA* **1999**, *96*, 6014 – 6019.
[54] S. O. Kelley, J. K. Barton, *Science* **1999**, *283*, 375 – 381.
[55] K. Fukui, K. Tanaka, M. Fujitsuka, A. Watanabe, O. Ito, *J. Photochem. Photobiol. B* **1999**, *50*, 18 – 24.
[56] F. D. Lewis, Y. Zhang, X. Liu, N. Xu, R. L. Letsinger, *J. Phys. Chem. B* **1999**, *103*, 2570 – 2578.
[57] S. O. Kelley, N. M. Jackson, M. G. Hill, J. K. Barton, *Angew. Chem.* **1999**, *111*, 991 – 996; *Angew. Chem. Int. Ed.* **1999**, *38*, 941 – 944.
[58] H. W. Fink, C. Schonenberger, *Nature* **1999**, *398*, 407 – 410.
[59] E. Meggers, M. E. Michel-Beyerle, B. Giese, *J. Am. Chem. Soc.* **1998**, *120*, 12950 – 12955.
[60] S. M. Gasper, G. B. Schuster, *J. Am. Chem. Soc.* **1997**, *119*, 12762 – 12771.
[61] B. Armitage, D. Ly, T. Koch, H. Frydenlund, H. Orum, H. G. Batz, G. B. Schuster, *Proc. Natl. Acad. Sci. USA* **1997**, *94*, 12320 – 12325.
[62] Y. Razskazovskii, S. G. Swartz, J. M. Falcone, C. Taylor, M. D. Sevilla, *J. Phys. Chem. B* **1997**, *101*, 1460 – 1467.
[63] D. Ly, Y. Kan, B. Armitage, G. B. Schuster, *J. Am. Chem. Soc.* **1996**, *118*, 8747 – 8748.
[64] I. Saito, T. Nakamura, K. Nakatani, Y. Yoshioka, K. Yamaguchi, H. Sugiyama, *J. Am. Chem. Soc.* **1998**, *120*, 12686 – 12687.
[65] M. E. Nunez, D. B. Hall, J. K. Barton, *Chem. Biol.* **1999**, *6*, 85 – 97.
[66] D. B. Hall, R. E. Holmlin, J. K. Barton, *Nature* **1996**, *382*, 731 – 735.
[67] D. B. Hall, J. K. Barton, *J. Am. Chem. Soc.* **1997**, *119*, 5045 – 5046.
[68] M. R. Arkin, E. D. A. Stemp, S. C. Pulver, J. K. Barton, *Chem. Biol.* **1997**, *4*, 389 – 400.
[69] S. R. Rajski, S. Kumar, R. J. Roberts, J. K. Barton, *J. Am. Chem. Soc.* **1999**, *121*, 5615 – 5616.
[70] D. B. Hall, S. O. Kelly, J. K. Barton, *Biochemistry* **1998**, *37*, 15933 – 15940.

  1433-7851/99/3824-3634 $ 17.50+.50/0

[71] B. Giese, S. Wessely, M. Spormann, U. Lindermann, E. Meggers, M. E. Michel-Beyerle, *Angew. Chem.* **1999**, *111*, 1050 – 1052; *Angew. Chem. Int. Ed.* **1999**, *38*, 996 – 998.
[72] E. Meggers, D. Kusch, M. Spichty, U. Wille, B. Giese, *Angew. Chem.* **1998**, *110*, 474 – 476; *Angew. Chem. Int. Ed.* **1998**, *37*, 460 – 462.
[73] D. T. Breslin, G. B. Schuster, *J. Am. Chem. Soc.* **1996**, *118*, 2311 – 2319.
[74] P. T. Henderson, D. Jones, G. Hampikian, Y. Kan, G. B. Schuster, *Proc. Natl. Acad. Sci. USA* **1999**, *96*, 8353 – 8358.
[75] D. J. Hurley, Y. Tor, *J. Am. Chem. Soc.* **1998**, *120*, 2194 – 2195.
[76] S. I. Khan, A. E. Beilstein, M. W. Grinstaff, *Inorg. Chem.* **1999**, *38*, 418 – 419.
[77] S. I. Khan, M. W. Grinstaff, *J. Am. Chem. Soc.* **1999**, *121*, 4704 – 4705.
[78] B. P. Hudson, J. K. Barton, *J. Am. Chem. Soc.* **1998**, *120*, 6877 – 6888.

Tyrosyl – tRNA Synthetase: A Housekeeping Protein and an Attractive Harbinger of Cellular Death

Hermann Schluesener*

Apoptosis, or programmed cell death, is a physiological process that occurs during tissue reorganization in embryonic development and pathological conditions. During execution of this cellular suicide program, nucleases fragment chromosomal DNA and activated proteases dismantle the cell by cleaving multiple substrates, including cytoskeletal proteins and enzymes that are essential for normal cellular function and cell repair.

Cells undergoing apoptosis are usually swiftly ingested by macrophages and this phagocytic clearance of intact apoptotic cells is a safe disposal route since local inflammatory reactions that result from a massive release of cellular debris are avoided. Furthermore, the ingestion of apoptotic cells by phagocytes may actively down-regulate local inflammatory and immune responses.[1]

Surprisingly, two novel signaling molecules of the apoptotic cascade have been described recently by Wakasuki and Schimmel.[2] These cytokines are fragments of tyrosyl – tRNA synthetase, an unsuspicious enzyme that is essential in protein synthesis (and consequently belongs to the housekeeping proteins). Cellular protein synthesis relies on a supramolecular organization of the mammalian translation system.[3] This protein-synthesizing machinery is a complex, but highly organized apparatus and the macromolecular components are not freely diffusible in mammalian cells. In particular, aminoacyl – tRNA appears to be channeled within the cell, that is, directly transferred from the aminoacyl – tRNA synthetases to the elongation factor, and then to the ribosomes, without dissociation into the cellular fluid.[4]

Functionally, human tyrosyl – tRNA synthetase is composed of a catalytic terminal amino domain and a terminal carboxy sequence. Approximately 50% of the terminal carboxy sequence is identical to the terminal carboxy region of the p43 protein, an auxiliary RNA binding factor of the mammalian multi-synthetase complex.[5]

[*] Prof. Dr. H. Schluesener
Institut für Hirnforschung der Universität
Calwer Strasse 3, D-72076 Tübingen (Germany)
Fax: (+49) 7071-29-5456
E-mail: hirnforschung@uni-tuebingen.de

During apoptosis, the translational apparatus is systematically destroyed. Interestingly, tyrosyl – tRNA synthetase is secreted from cells undergoing apoptosis. After cleavage by elastase or related proteases, two fragments with surprisingly novel bioactivities are generated (Figure 1). Both fragments

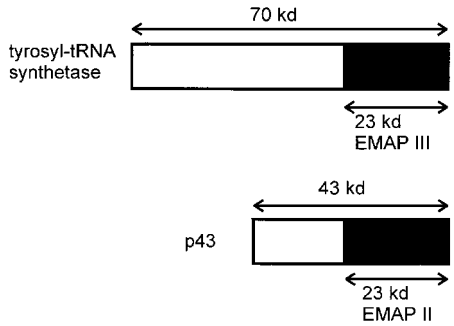

Figure 1. Tyrosyl – tRNA synthetase and the auxiliary p43 protein are cleaved by elastase or related proteases (such as caspases or multicatalytic protease) into two fragments. The terminal carboxy fragments EMAP II and III are homologous modulators of leukocyte migration and activation.

appear to act as local signaling molecules (cytokines) that orchestrate the tissue response and culminate in the safe removal of apoptotic cells.

Tyrosyl – tRNA Synthetase: Surprising Bioactivities of Cleavage Products

Full-length tyrosyl – tRNA synthetase has no effect on leukocytes, but both fragments are potent leukocytic activators with different spectra of bioactivities.[2] The catalytic aminoterminal domain contains an Glu-Ag-Leu (ERL) sequence motif, which is characteristic of certain chemokines, a family of chemoattractant cytokines. It has been shown that the aminoterminal peptide of tyrosyl – tRNA synthetase binds to the interleukin-8 (IL-8) receptor type A (also known as CXCR1). Subsequent bioassays showed that this peptide has IL-8 activity, predominantly by activating and inducing migration of neutrophilic granulocytes.[2]

  1433-7851/99/3824-3635 $ 17.50+.50/0